Dissociation of molecular oxygen on unpromoted and cesium-promoted Ag(111) surfaces

Michael R. Salazar *, Joel D. Kress and Antonio Redondo

Theoretical Division, Group T-12, Los Alamos National Laboratory, Los Alamos, NM 87545, USA
E-mail: salazarm@lanl.gov

Received 9 August 1999; accepted 30 November 1999

Density functional calculations for the dissociation of molecular oxygen on a Ag_{10} cluster model (seven surface and three subsurface atoms) of the [111] surface of silver are presented. The calculations show that the reaction pathway for the dissociation of molecular oxygen depends on the amount of cesium present on the surface. For the unpromoted surface, dissociation should have a low rate as the process is activated. As a single Cs atom is added to the cluster, O_2 should readily dissociate since the process is kinetically and thermochemically favored. However, as a second Cs atom is added, the dissociation of O_2 is quenched as the process is highly activated.

Keywords: O_2 dissociation on Ag, thermochemistry, density functional theory calculations, olefin epoxidation

The interplay between the chemisorption and dissociation of O_2 on silver-based catalysts is of considerable importance in understanding the mechanism of olefin epoxidation and in suggesting possible methods of improving the catalytic properties of this important class of industrial catalysts. Because olefins are often the starting point for making commodity products, it is desirable to make the processes to oxidize olefins fast, efficient, and highly selective. A commercially important avenue for accomplishing these goals is the partial oxidation of olefins on silver-based catalysts. In particular, the oxidation of ethylene on Ag catalysts has received much experimental and theoretical study [1–23]. In spite of this attention, there are a number of differing opinions regarding the oxygen species on Ag [1,2,6,7,10,11] and this ambiguity is further complicated when electron-donating and electron-withdrawing atoms are added to the Ag surface. These electron-donating and electron-withdrawing atoms are referred to as promoters. It has been shown experimentally that these promoters can have a large effect on the catalytic properties of the Ag surface [13–23]. If one could elucidate the role of these promoters, then it is possible to suggest optimum promoter types and coverages, so that the Ag catalyst gives the best possible selectivity and activity toward olefin epoxidation.

The interaction of oxygen with Ag surfaces has been the subject of other theoretical investigations [24–31]. Most of this work has focused on the [110] face of Ag, while leaving the [111] face relatively unstudied. There have also been scattering experiments [32–34], temperature desorption experiments [7], and spectroscopic experiments [35] aimed at elucidating the potential energy diagram for various states of oxygen on Ag.

We have investigated, with density functional theory, energetic pathways for the dissociation of O_2 on a ten-atom cluster representative of the (111) surface of silver. This ten-atom cluster model, illustrated in figure 1, contains seven surface Ag atoms and three second-layer Ag atoms. The surface binding sites are also illustrated in figure 1. The *three-fold* binding sites have a second-layer Ag atom directly beneath them (sites A, C, and E in figure 1), while the *three-fold hollow* binding sites are without a second-layer Ag atom directly beneath them (sites B, D, and F in

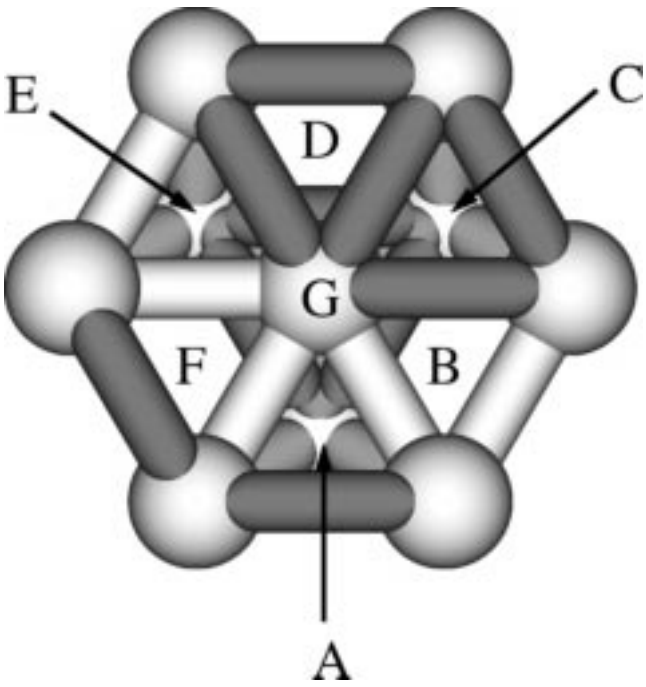

Figure 1. Ag_{10} cluster and the surface binding sites.

* To whom correspondence should be addressed.

figure 1). In all the calculations, the Ag cluster was held fixed, using the bulk Ag–Ag distance [36] of 2.89 Å, and not allowed to relax when species adsorbed. In addition to adding molecular oxygen to the surface, we have added one and two Cs atoms to the surface of the cluster and repeated the search for dissociation pathways. In this letter we report those pathways that form the lowest energy dissociated products on the unpromoted, singly, and doubly promoted Ag cluster models.

Electronic structure calculations were carried out using density functional theory, with the gradient-corrected Becke exchange [37] and the Lee–Yang–Parr correlation functionals [38] (B3LYP). The Gaussian '98 suite of programs was used for all calculations [39]. The core electrons of silver and cesium were replaced by effective core potentials. For Cs we used the LANL2 effective core potential [40]. This potential replaces the 46 inner shell electrons of cesium and treats the 9 outer shell ($5s^25p^66s^1$) electrons explicitly. A corresponding double-zeta (DZ) basis set, containing 12 basis functions, was used for these outer shell electrons. For the Ag atom, the LANL1 [41] effective core potential, along with a 9 basis function minimum basis (MB) set, was used. The LANL1 effective core potentials replace the 36 inner shell electrons and treat the 11 outer shell ($4d^{10}5s^1$) electrons explicitly. For oxygen, a 6-31 + G* basis set was used, which consists of a double-zeta valence basis set with polarization and diffuse functions [39]. For all calculations reported herein, we investigated many different spin states. The values reported are for the lowest energy spin states.

Shown in figure 2 are the reaction pathways that form the lowest energy dissociative products. The hexagonal structure shown in this figure is a wire-frame diagram of the Ag_{10} cluster model. The seven Ag surface atoms are located at the apices and center of the hexagon and the three second-layer atoms are illustrated by the dots inside the hexagonal structure. Reactions (A), (B), and (C) in figure 2 show the pathways to form the lowest energy dissociative products on the unpromoted, singly, and doubly promoted cluster models, respectively.

Starting at the right-hand side (RHS) of reaction (A) in figure 2, the adsorption of O_2 onto the Ag cluster is bound by 20.4 kcal/mol. Both the singlet and triplet spin states were investigated. We found that the triplet state was the lowest energy state, but the singlet sate was 12.6 kcal/mol higher in energy. The O_2 prefers to bind to the three-fold hollow site, but O_2 binding to the three-fold site (not shown in figure 2(A)) is only slightly less stable by ∼2 kcal/mol relative to the three-fold hollow site. Once molecular oxygen is bound to the three-fold hollow site, it may dissociate to form oxygen atoms on the surface. The lowest energy configuration, for two O atoms on a single cluster, is when both oxygen atoms reside in separate three-fold hollow sites. This configuration lies 6.8 kcal/mol higher than the adsorbed state. The barrier for this pathway is ∼24 kcal/mol, which is ∼4 kcal/mol higher than the desorbed O_2 asymptote. The O–O distance for the transition state is 1.78 Å (compared to 1.21 Å in gas-phase O_2) and both oxygen atoms are at approximately the same distance (1.68 Å) from the surface. Continuing along the reaction coordinate in figure 2(A), we find that two O atoms on the Ag_{10} cluster repel each other (by 39.8 kcal/mol) compared to twice the energy of a single O atom binding to a three-fold hollow site on the Ag_{10} cluster. This state is 33.0 kcal/mol below the adsorbed O_2 state and 53.4 kcal/mol below the desorbed asymptote. Both O atoms reside in three-fold hollow sites and are at a distance of 1.41 Å from the surface.

Although our cluster calculations do not include subsurface oxygen, we compare in table 1 our calculated energies for species along the dissociative pathway of the unpromoted cluster model with the experimental results of Campbell [7] and Raukema et al. [33]. As seen in this table, the calculated values are in fair agreement with the experimental results. We did not attempt to calculate the weak barrier to chemisorption because we judged the uncertainty to be higher, relative to the other calculations reported in the table. Our calculated binding energy for molecular oxygen is larger than the experimental values by ∼7–11 kcal/mol, a difference that may be partly ascribable to the lack of subsurface oxygen and the finite size of our clusters. This trend is consistent with other calculations we have carried out where the minimum basis set of silver is used in conjunction with the 6-31 + G* basis for oxygen. We will report elsewhere comparisons between silver minimum and double-zeta basis sets that show this trend [42]. The third row of table 1 shows excellent agreement between our calculated activation barrier for dissociation of O_2 and the experimental values. Shown in the fourth row is the binding energy of atomic O adsorption. Our calculated value agrees well with one experiment and is within 14 kcal/mol of the other. Again the minimum basis set on silver tends to overbind oxygen (53.4 kcal/mol) compared to a binding energy of 25.7 kcal/mol obtained when the double-zeta basis set is used on the silver atoms.

The reactive pathway for the dissociation of O_2 on a cluster model containing one Cs is illustrated in reaction (B) of figure 2. This model represents a "low" coverage of cesium. Starting at the RHS of this figure, the binding energy of O_2 is 28.8 kcal/mol when the Cs and O_2 molecule each occupy three-fold sites. Both the doublet and quartet spin states were investigated for this promoted cluster. We found that the doublet state was the lowest energy spin state (the quartet was ∼6 kcal/mol above the doublet). The lowest energy product formed by the dissociation of O_2, via the motion of a single oxygen atom to another site, is the Cs (three-fold)/O (three-fold)/O (three-fold hollow) configuration. This product state is 14.3 kcal/mol lower in energy than the adsorbed O_2 initial state. The barrier between the adsorbed O_2 initial configuration and this dissociation product is ∼17 kcal/mol above the adsorbed state; however, this transition state is ∼11 kcal/mol below the desorbed O_2 asymptote. The O–O distance for this transition state is 2.25 Å. The dissociated product state may lower the energy of the system by an additional 6.1 kcal/mol by moving the

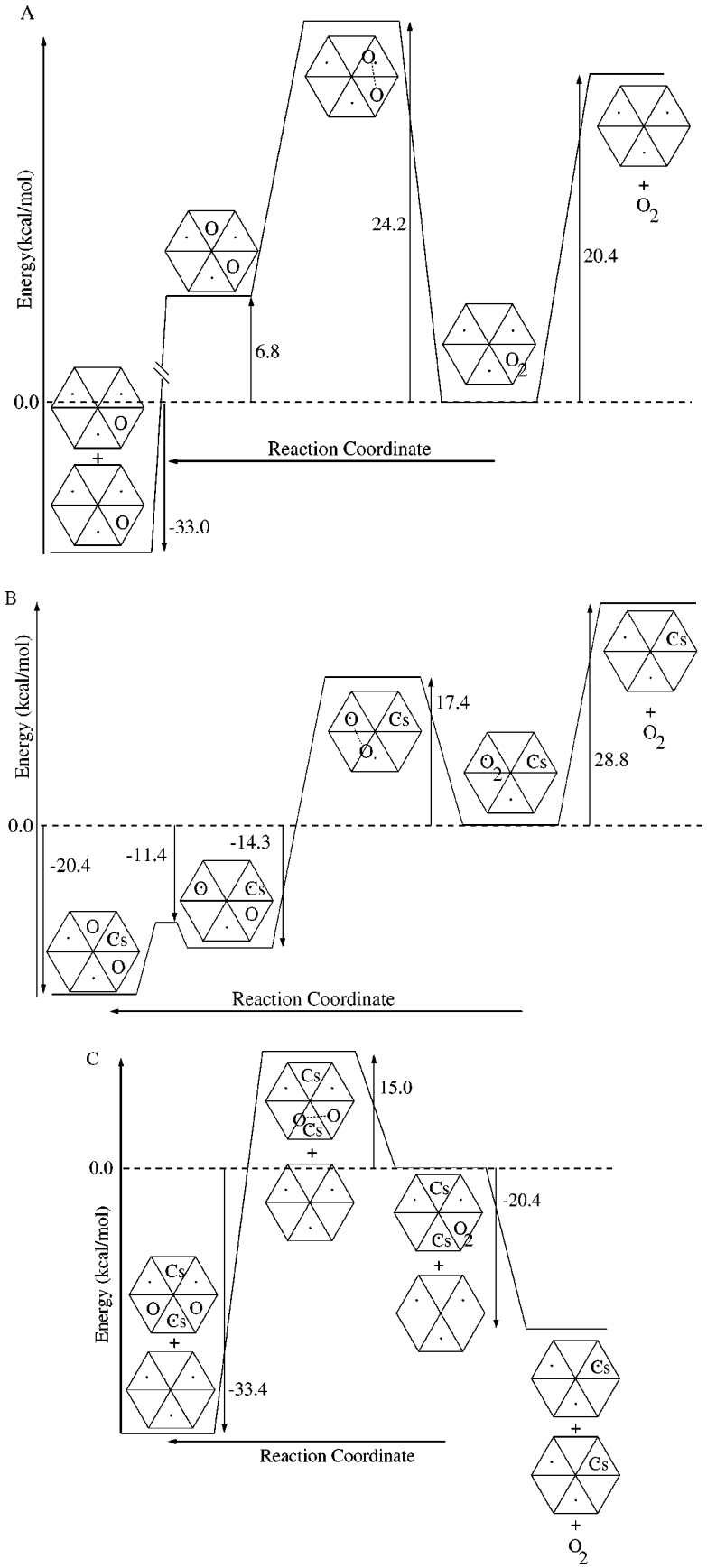

Figure 2. Energy diagrams for the dissociation of O_2 on the unpromoted, singly, and doubly promoted Ag_{10} clusters. The dots inside the hexagonal Ag cluster indicate where the bottom layer of Ag atoms reside.

Table 1
Comparison of the calculated and experimentally determined energetic values for the species along the O_2 dissociation pathway.[a]

Species	Campbell[b]	Raukema et al.[c]	Present results[d]
Chemisorption barrier	3.2	5.8	–
O_2 chemisorption	−9.2	-12.9 ± 0.9	−20.4
Activation barrier	−0.9	3.9 ± 0.9	3.8
O/O adsorption	−40.8	-54.0 ± 10.4	−53.4

[a] All energies relative to the desorbed O_2 asymptote.
[b] [7].
[c] [33].
[d] LANL1MB effective core potential/minimum basis set is used on the Ag atoms.

three-fold oxygen to the three-fold hollow site next to the Cs atom. The barrier to accomplish this is ∼3 kcal/mol higher than the original dissociated product state.

We next added, besides oxygen, two Cs atoms to the Ag_{10} cluster and sought dissociative pathways. We found that when two Cs atoms were added to the Ag_{10} cluster, without any oxygen, that this complex was unstable and one of the Cs atoms desorbed. However, when oxygen (in the form of O_2 or adsorbed O atoms) was on the cluster, both Cs atoms were bound to the surface. These calculations are in agreement with experiment: that the presence of oxygen on a promoted silver catalyst allows for higher coverages of cesium by forming oxides of Cs [17,18]. This suggests that when a thermally stable, cesium-promoted catalyst is exposed to O_2, Cs atoms will migrate along the silver surface to positions near the oxygen, thus opening up additional binding sites for more cesium.

In reaction (C) of figure 2, the dissociative pathway for the Ag cluster with two adsorbed Cs atoms is illustrated. This model represents a "high" coverage of cesium. Starting at the RHS of this reactive pathway, the desorbed O_2 asymptote has two Ag clusters with each containing a single Cs atom. This asymptote is used because two Cs atoms adsorbed on a single Ag_{10} cluster are unstable with respect to the desorption of one of the Cs atoms. When the O_2 molecule and both Cs atoms adsorb to one of the Ag_{10} clusters, we obtain a bound state whose energy is 20.4 kcal/mol higher than the desorbed O_2 asymptote. For the doubly promoted cluster, the adsorbed O_2 lowest energy configuration occurs when the Cs atoms occupy opposing three-fold and three-fold hollow sites, while the oxygen occupies a three-fold hollow site. We investigated both the singlet and triplet spin states for this doubly promoted cluster. We found that the singlet spin state was the lowest energy state – the triplet was ∼2 kcal/mol higher. This initial configuration of O_2 may dissociate to form the lowest energy dissociated product state by moving a single oxygen atom. This state is obtained when the oxygen atom that is farthest above the Ag surface moves to the three-fold hollow site neighboring the three-fold Cs atom. This product state is 33.4 and 13.0 kcal/mol lower in energy than the adsorbed O_2 configuration and the desorbed O_2 asymptote, respectively. The transition state connecting the initial adsorbed O_2 state with the dissociated product state has a barrier that is ∼15 kcal/mol higher than the initial state. The O–O distance is 1.94 Å at the transition state.

Table 2
Comparison of reaction thermochemistry and barrier heights for the LANL1MB and LANL1DZ basis sets (each with LANL1MB geometries).

Reaction	Barrier heights (kcal/mol)		Product energies (kcal/mol)	
	LANL1MB	LANL1DZ	LANL1MB	LANL1DZ
Unpromoted	24.2	30.0	−33.0	−18.2
Singly promoted	17.4	21.6	−14.3	−11.9
Doubly promoted	15.0	14.4	−33.4	−28.6

To check the dependence of the thermochemical quantities on the quality of the basis sets we have recomputed all the reactant and product energies as well as the barrier heights using the larger double-zeta (DZ) basis set for silver at the minimum basis (MB) set geometries. Shown in table 2 are the MB and DZ energies of the barrier heights (columns 2 and 3) and product energies (columns 4 and 5), relative to the Ag_{10} cluster with adsorbed cesium and O_2. For the unpromoted cluster, the barrier heights for the double-zeta basis are increased by ∼6 kcal/mol with respect to those calculated with the minimum basis set, while the product energies are increased by ∼14 kcal/mol. The singly promoted cluster has barrier heights and product energies that are increased by ∼5 and 3–6 kcal/mol, respectively, in going from the MB to the DZ basis. The doubly promoted cluster has the smallest differences in the MB and DZ energies as the barrier heights and product energies differed by ∼1 and ∼0.5 to ∼5 kcal/mol, respectively. The examination of the energetics of table 2 reveals that increasing the size of the Ag basis set tended to increase the barrier heights and product energies. The conclusions drawn from the MB energetics are not affected, because the barrier heights and product energies remained with the same relative orderings and differences in going from the minimum basis set to the double-zeta basis set. Also seen in table 2 is that the differences between the MB and DZ basis set get smaller as one adds cesium atoms. This decreasing difference in the energies may be understood as the basis sets on the cesium atoms help compensate for the lack of flexibility present in the silver minimum basis set.

In addition to examining the effect of the basis set on the results, we also investigated the effect of larger cluster models [42]. For example, the binding of Cs is changed by less than ∼2 kcal/mol with a larger Ag_{15} cluster model, relative to the present Ag_{10} cluster model. The chemisorption of molecular oxygen shows the largest change in binding energy with cluster size. We compute a decrease in the binding energy of ∼10 kcal/mol, relative to the results of the Ag_{10} cluster. However, the energy difference between the atomic and molecular chemisorbed states in the Ag_{10} and Ag_{15} clusters is ∼3 kcal/mol. It is these energy differences between the two cluster models that is most important for predicting the properties of oxygen on Ag.

Figure 2 illustrates the reaction pathways to form the lowest energy product states for the unpromoted, singly, and

doubly promoted Ag_{10} cluster. O_2 dissociation on the unpromoted cluster (reaction (A)) is kinetically unfavored but thermochemically favored, in agreement with experiment (see table 1). These results suggest a low rate of O_2 dissociation on the clean unoxidized (111) surface. With the addition of a single Cs atom to the cluster (reaction (B)), a very different outcome is predicted by our calculations. For the singly promoted cluster, the dissociation of O_2 is kinetically and thermochemically favored; thus, for low coverages of Cs on bulk unoxidized Ag(111) surfaces, these calculations suggest that molecular oxygen will readily dissociate. The calculations on the doubly promoted cluster model (reaction (C)) demonstrate that dissociation is kinetically unfavored, but thermochemically favored. The calculated barrier for dissociation is sufficiently large ($\sim$35 kcal/mol from desorbed O_2 to the transition state) that we would not expect much O_2 to dissociate under typical catalytic temperatures ($\sim$250 °C). Thus, according to these calculations, the dissociation of O_2 on bulk Ag(111) is expected to exhibit the following pattern: for the unpromoted surface, dissociation should have a low rate as the process is activated. However, as Cs is added to the catalyst, O_2 should readily dissociate; but, as even more Cs is added (resulting in high Cs coverages), the dissociation of O_2 will be slowly diminished. These results show a large Cs coverage dependence on the dissociation of O_2. A similar effect has been shown for the dissociation of N_2 on Ru with Cs promotion [43]. Although more work remains to be done before a definitive answer can be given regarding how low coverages of Cs promote the dissociation of O_2, preliminary results suggest that it is due to the donation of the Cs valence electron into the π^* orbital of O_2, thus increasing the negative charge on the O_2 and decreasing the bond order.

When our results on O_2 dissociation as a function of cesium coverage are compared with the experimentally observed selectivity of ethylene oxide, a complementary pattern is observed. Experimentally it has been observed that the selectivity of forming ethylene oxide falls as Cs is added to an unpromoted Ag surface, but, as more Cs is added, the selectivity rises again until it surpasses the selectivity for the unpromoted surface [17]. This may suggest a correlation between the presence of undissociated molecular oxygen and the selectivity to ethylene oxide formation.

Acknowledgement

The authors wish to thank Drs. John Monnier, Eric Middlemas, Bruce Wilson, and Chandra Saravanan for enlightening discussions. This work has been carried out with support from Eastman Chemical Company and the United States Department of Energy (under contract W-7405-ENG-36).

References

[1] R.B. Clarkson and A.C. Cirillo, Jr., J. Vac. Sci. Technol. 9 (1972) 1073.
[2] P.A. Kilty and W.M.H. Sachtler, Catal. Rev. Sci. Eng. 10 (1974) 1.
[3] N.W. Cant and W.K.J. Hall, J. Catal. 52 (1978) 81.
[4] M. Akimoto, K. Ichikawa and E. Echigoya, J. Catal. 76 (1982) 333.
[5] P.V. Geenen, H.J. Boss and G.T. Pott, J. Catal. 77 (1982) 499.
[6] C.T. Campbell, J. Catal. 94 (1985) 436.
[7] C.T. Campbell, Surf. Sci. 157 (1985) 43.
[8] H. Nakatsuji, Z. Hu and H. Nakai, Int. J. Quantum Chem. 65 (1997) 839.
[9] R.B. Grant and R.M. Lambert, J. Catal. 92 (1985) 364.
[10] R.A. van Santen and C.P.M. De Groot, J. Catal. 98 (1986) 530.
[11] E.A. Carter and W.A. Goddard, J. Catal. 112 (1988) 80.
[12] J.T. Gleaves, A.G. Sault, R.J. Madix and J.R. Ebner, J. Catal. 121 (1990) 202.
[13] P. Yinsheng, Z. Shi, T. Liang and D. Jingfa, Catal. Lett. 12 (1992) 307.
[14] C.J. Bertole and C.A. Mims, J. Catal. 184 (1999) 224.
[15] M. Kitson and R.M. Lambert, Surf. Sci. 109 (1981) 60.
[16] C.T. Campbell and B.E. Koel, J. Catal. 92 (1985) 272.
[17] C.T. Campbell, J. Phys. Chem. 89 (1985) 5789.
[18] R.B. Grant and R.M. Lambert, Langmuir 1 (1985) 29.
[19] C.T. Campbell, J. Catal. 99 (1986) 28.
[20] S.A. Tan, R.B. Grant and R.M. Lambert, J. Catal. 106 (1987) 54.
[21] M. Dean, A. McKee and M. Bowker, Surf. Sci. 211/212 (1989) 1061.
[22] D. Jingfa, Y. Jun, Z. Shi and Y. Xiaohong, J. Catal. 138 (1992) 395.
[23] Ch. Karavasilis, S. Bebelis and C.G. Vayenas, J. Catal. 160 (1996) 205.
[24] K. Broomfield and R.M. Lambert, Mol. Phys. 66 (1989) 421.
[25] E.A. Carter and W.A. Goddard, Surf. Sci. 209 (1989) 243.
[26] H. Nakatsuji and H. Nakai, Chem. Phys. Lett. 174 (1990) 283.
[27] H. Nakatsuji and H. Nakai, J. Chem. Phys. 98 (1993) 2423.
[28] P.A. Gravil, J.A. White and D.M. Bird, Surf. Sci. 352–354 (1996) 248.
[29] P.A. Gravil, D.M. Bird and J.A. White, Phys. Rev. Lett. 77 (1996) 3933.
[30] D.M. Bird and P.A. Gravil, Surf. Sci. 377–379 (1997) 555.
[31] V.I. Avdeev, S.F. Ruzankin and G.M. Zhidomirov, J. Struct. Chem. 38 (1997) 519.
[32] A.W. Kleyn, D.A. Butler and A. Raukema, Surf. Sci. 363 (1996) 29.
[33] A. Raukema, D.A. Butler, F.M.A. Box and A.W. Kleyn, Surf. Sci. 347 (1996) 151.
[34] A. Raukema, D.A. Butler and A.W. Kleyn, J. Chem. Phys. 106 (1997) 2477.
[35] L. Vattuone, M. Rocca and U. Valbusa, Surf. Sci. 314 (1994) L904.
[36] L.E. Sutton, *Tables of Interatomic Distances and Configuration in Molecules and Ions* (Royal Society of Chemistry, London, 1965).
[37] A.D. Becke, J. Chem. Phys. 98 (1993) 5648.
[38] C. Lee, W. Yang and R.G. Parr, Phys. Rev. B 37 (1988) 785;
B. Miehlich, A. Savin, H. Stoll and H. Preuss, Chem. Phys. Lett. 157 (1989) 200.
[39] M.J. Frisch et al., Gaussian '98, Revision A.6, Gaussian Inc., Pittsburgh, PA, 1998.
[40] P.J. Hay and W.R. Wadt, J. Chem. Phys. 82 (1985) 299.
[41] P.J. Hay and W.R. Wadt, J. Chem. Phys. 82 (1985) 270.
[42] C. Saravanan, J.D. Kress, M.R. Salazar and A. Redondo, to be published;
M.R. Salazar, C. Saravanan, J.D. Kress and A. Redondo, to be published.
[43] J.J. Mortensen, B. Hammer and J.K. Norskov, Phys. Rev. Lett. 80 (1998) 4333.